DOI: 10.11844/cjcb.2025.12.0016
中国细胞生物学学报 Chinese Journal of Cell Biology 2025, 47(12): 3182–3191 CSTR: 32200.14.cjcb.2025.12.0016

LncRNA MIR17HG靶向miR-153-3p对骨髓瘤细胞增殖、侵袭的影响

安宏玉 张欣*
(黄石市中心医院血液内科, 黄石 435000)

摘要 该文旨在探讨LncRNA MIR17HG靶向miR-153-3p对骨髓瘤(MM)细胞增殖、侵袭的影响。qRT-PCR检测MM组织、正常骨髓组织、人正常骨髓浆细胞(nPCs)和MM细胞(U266、RPMI-8226、NCI-H929、LP-1)中MIR17HG和miR-153-3p的表达水平; 将NCI-H929细胞分为control组、si-NC组、si-MIR17HG组、si-MIR17HG+inhibitor NC组、si-MIR17HG+miR-153-3p inhibitor组、si-MIR17HG+miR-NC组, si-MIR17HG+miR-153-3p mimics组; qRT-PCR检测细胞中MIR17HG、miR-153-3p表达水平; CCK-8检测细胞增殖; 划痕实验检测细胞迁移; Transwell实验检测细胞侵袭; 流式细胞术检测细胞凋亡; Western blot检测细胞中E-cadherin、cleaved caspase-3、N-cadherin、vimentin、PCNA、MMP-2蛋白表达水平; 双荧光素酶活性实验验证miR-153-3p与MIR17HG的靶向关系。MM组织和MM细胞系中MIR17HG表达水平升高, miR-153-3p表达水平降低; 敲低MIR17HG表达后NCI-H929细胞中MIR17HG表达水平下降, D_{450}(24 h、48 h)值降低, 划痕愈合率降低, N-cadherin、vimentin、PCNA和MMP-2蛋白表达水平降低, 细胞侵袭数量减少, miR-153-3p表达水平, 凋亡率, E-cadherin和cleaved caspase-3蛋白表达水平升高(P<0.05); 沉默miR-153-3p表达可降低敲低MIR17HG表达对NCI-H929细胞恶性生物学行为的抑制作用(P<0.05); 上调miR-153-3p表达可提高敲低MIR17HG表达对NCI-H929细胞恶性生物学行为的抑制作用(P<0.05)。MIR17HG可调控miR-153-3p表达影响MM细胞恶性生物学行为。

关键词 MIR17HG; miR-153-3p; 骨髓瘤; 增殖; 侵袭

Impacts of LncRNA MIR17HG on Proliferation and Invasion of Myeloma Cells by Targeting miR-153-3p

AN Hongyu, ZHANG Xin*
(*Department of Hematology, Huangshi Central Hospital, Huangshi 435000, China*)

Abstract This article aims to explore the effects of LncRNA MIR17HG targeting miR-153-3p on the proliferation and invasion of MM (myeloma) cells. qRT-PCR method was used to detect MIR17HG and miR-153-3p in MM tissue, normal bone marrow tissue, nPCs (human normal bone marrow plasma cells), and MM cells (U266, RPMI-8226, NCI-H929, LP-1). NCI-H929 cells were assigned into control group, si-NC group, si-MIR17HG group, si-MIR17HG+inhibitor NC group, si-MIR17HG+miR-153-3p inhibitor group, si-MIR17HG+miR-NC group, and si-MIR17HG+miR-153-3p mimics group. qRT-PCR was performed to determine the expression levels of MIR17HG and miR-153-3p in cells. The CCK-8 assay was conducted to assess cell proliferation. A wound heal-

收稿日期: 2025-07-11 接受日期: 2025-10-16
湖北省科学技术厅自然科学基金(批准号: 2022CFB797)资助的课题
*通信作者。Tel: 13687182363, E-mail: muoae2@163.com
Received: July 11, 2025 Accepted: October 16, 2025
This work was supported by the Hubei Provincial Natural Science Foundation Project (Grant No.2022CFB797)
*Corresponding author. Tel: +86-13687182363, E-mail: muoae2@163.com

ing assay was used to evaluate cell migration. A Transwell assay was carried out to examine cell invasion. Flow cytometry was employed to detect cell apoptosis. Western blot was used to detect the protein expression levels of E-cadherin, cleaved caspase-3, N-cadherin, vimentin, PCNA, and MMP-2 in cells. The targeting relationship between miR-153-3p and MIR17HG was validated. The MIR17HG increased and miR-153-3p decreased in MM tissues and MM cell lines. After knockdown of MIR17HG expression, the expression level of MIR17HG in the NCI-H929 cells, the values of D_{450} (24 h, 48 h) , the scratch healing rate, the protein expression levels of N-cadherin, vimentin, PCNA and MMP-2 , and the number of cell invasions reduced, while the expression level of miR-153-3p, apoptosis rate, the protein expression levels of E-cadherin, and cleaved caspase-3 increased (P<0.05). Silencing miR-153-3p could reduce the inhibitory effect of knocking down MIR17HG on the malignant biological behaviors of NCI-H929 cells (P<0.05). Moreover, upregulation of miR-153-3p could enhance the inhibitory effect of knocking down MIR17HG on the malignant biological behaviors of NCI-H929 cells (P<0.05). MIR17HG can regulate the expression of miR-153-3p and affect the malignant biological behavior of MM cells.

Keywords MIR17HG; miR-153-3p; myeloma; proliferation; invasion

多发性骨髓瘤(myeloma, MM)是一种血液系统恶性肿瘤, 其特征是骨髓浆细胞异常增殖影响正常的造血功能[1]。MM是全世界最常见的血液肿瘤, 在血液系统恶性肿瘤中占比约为13%, 其发病率和死亡率居高不下[2]。在临床治疗中, MM的治疗方案通常涵盖化疗、自体/同种异体干细胞移植和靶向治疗, 然而, MM的临床治疗效果仍不理想。目前, MM的发病机制尚不明确, 从分子水平解析MM的发生及细胞迁移机制, 对探索靶向干预策略以改善患者预后具有重要价值[3]。研究显示, LncRNA参与肿瘤进展的调控[4]。MIR17HG在骨髓瘤细胞中高表达, 具有致癌功能[5]。MIR17HG在肺癌细胞中高表达, 下调MIR17HG表达可降低肺癌细胞致瘤性, 抑制细胞免疫逃逸[6]。LncRNA对肿瘤细胞生物学活性的影响, 是通过调控其下游靶miRNA的表达来实现的[7]。miR-153-3p在食管癌中低表达, 上调miR-153-3p表达可抑制食管癌细胞增殖、迁移和侵袭[8]。提高miR-153-3p表达可阻滞甲状腺癌细胞周期, 促进细胞凋亡, 抑制其增殖、迁移和糖酵解[9]。推测miR-153-3p高表达可抑制肿瘤细胞恶性生物学行为。Starbase网站预测分析发现miR-153-3p与MIR17HG存在靶向位点。基于此, 本研究旨在探讨MIR17HG对MM细胞生物学活性的影响, 并验证其调控作用是否通过靶向miR-153-3p来实现的。

1 材料与方法

1.1 材料

1.1.1 组织与细胞 收集黄石市中心医院接受治疗的26例MM患者的骨髓组织和26例同期进行骨髓穿刺但最后确认为非MM患者的骨髓组织(2022年5月至2024年4月)。已将相关研究事宜告知所有患者, 黄石市中心医院伦理委员会已批准与授权, 批准号为2022-017。

人正常骨髓浆细胞(nPCs)和MM细胞(U266、RPMI-8226、NCI-H929、LP-1)购自上海乾思生物科技有限公司。

1.1.2 试剂与仪器 inhibitor NC、miR-153-3p inhibitor、si-NC、si-MIR17HG、miR-NC、miR-153-3p mimics质粒购自上海博尔森生物科技有限公司; 细胞凋亡检测试剂盒、qRT-PCR试剂盒、CCK-8试剂盒、蛋白提取试剂盒、双荧光素酶试剂盒和Transwell小室购自上海派森诺生物科技股份有限公司; vimentin、β-actin、E-cadherin、cleaved caspase-3、MMP-2、PCNA、N-cadherin抗体和二抗IGG购自上海艾博抗贸易有限公司; Feyond-A300多功能酶标仪购自杭州奥盛仪器有限公司; C7荧光定量PCR仪购自北京同洲维普科技有限公司; FACSCanto II流式细胞仪购自北京北嘉美仪生物科技有限公司。

1.2 方法

1.2.1 MIR17HG、miR-153-3p表达检测 采用RNA提取试剂盒提取组织及细胞总RNA, 经逆转录试剂盒合成cDNA后, 行qRT-PCR扩增。引物序列如下: MIR17HG上游序列为5′-GGC GTC CCG TCG TAG TAA AG-3′, 下游序列为5′-CAT TGT GTC AGG AGT CAG TGT GTC-3′; miR-153-3p上游序列为

5′-TTG CAT AGT CAC AAA AGT GAT C-3′, 下游序列为5′-GAT CAC TTT TGT GAC TAT GCA A-3′; *U6*上游序列为5′-TGC GGG TGC TCG CTT CGC AGC-3′, 下游序列为5′-CCA GTG CAG GGT CCG AGG T-3′; *β-actin*上游序列为5′-ATC ATG TTT GAG ACC TTC AAC A-3′, 下游序列为5′-CAT CTC TTG CTC GAA GTC CA-3′。以$2^{-\Delta\Delta Ct}$法计算基因表达水平。

1.2.2 分组 将NCI-H929细胞进行分组, 标记为control组、si-NC组、si-MIR17HG组、si-MIR17HG+inhibitor NC组、si-MIR17HG+miR-153-3p inhibitor组、si-MIR17HG+miR-NC组, si-MIR17HG+miR-153-3p mimics组, 将相应质粒转入相对应组的NCI-H929细胞中。转染完成后于37 ℃、5% CO_2的恒温培养箱中培养24 h进行后续实验。

1.2.3 细胞增殖检测 将NCI-H929细胞接种于96孔板(4×10^3/孔), 于37 ℃、5% CO_2的恒温培养箱中正常培养, 在时间点(24 h和48 h)时每孔加入10 μL CCK-8溶液, 于37 ℃孵育2 h后, 酶标仪检测450 nm处*D*值。

1.2.4 细胞迁移分析 将处于对数生长期的NCI-H929细胞以每孔2×10^5个的密度接种于6孔板中。待细胞生长至约90%融合度时, 使用无菌枪头在单层细胞表面制造一条直线划痕, 立即于显微镜下记录0 h的划痕宽度。更换为无血清培养基后, 将细胞放回培养箱继续培养。在划痕制造24 h后, 再次于相同位置拍摄照片并测量划痕宽度。最终通过比较0 h与24 h的划痕宽度数据, 计算划痕愈合率。

1.2.5 细胞侵袭检测 用无血清培养基将NCI-H929细胞浓度调整为5×10^5/mL, 将Matrigel基质胶用该培养基进行稀释后, 用以包被Transwell上室。随后, 向上室中加入100 μL细胞悬液, 同时向下室加入600 μL含有血清的培养基。24 h培养结束后, 对小室内的细胞进行4%多聚甲醛固定处理, 室温条件下持续20 min。待固定完成后进行染色处理, 之后在显微镜下观察细胞侵袭的情况。

1.2.6 细胞凋亡检测 1 000 ×*g*、4 ℃离心各组NCI-H929细胞5 min, 收集NCI-H929细胞并制备成密度为1×10^6/mL的单细胞悬液。随后, 取100 μL细胞悬液与5 μL Annexin V-FITC及5 μL PI染液充分混合, 构成染色工作液, 于室温条件避光孵育15 min, 最后, 使用流式细胞仪对样本进行检测, 以分析细胞凋亡情况。

1.2.7 蛋白表达分析 提取NCI-H929细胞总蛋白, BCA法检测蛋白浓度, 95 ℃热水将蛋白变性, 取15 μL样品加入电泳槽电泳, 将蛋白样品转印至PVDF膜后, 用5%脱脂牛奶室温封闭2 h。随后加入以下兔源一抗: MMP-2、cleaved caspase-3、E-cadherin、PCNA、β-actin、N-cadherin及vimentin(1∶1 500), 4 ℃孵育过夜。洗膜后, 加入相应二抗(1∶5 000)室温孵育2 h, ECL化学发光试剂进行显影后通过Image-Pro Plus软件对目标条带的灰度值进行定量分析。

1.2.8 分析MIR17HG与miR-153-3p的靶向关系 将miR-NC和miR-153-3p mimics分别与MIR17HG野生型(MIR17HG-WT)和突变型载体(MIR17HG-MUT)共转染到NCI-H929细胞中, 转染48 h后进进行荧光素酶活性检测。

1.3 统计分析

有实验数据均采用Shapiro-Wilk检验进行正态性分析, 结果显示各组数据均符合正态分布; 采用Levene检验进行方差齐性分析, 结果显示各组数据方差齐性, 实验数据均以均值±标准差($\bar{x}\pm s$)表示。采用GraphPad Prism 8.0.1软件进行所有统计分析。两组间比较采用独立样本*t*检验; 多组间比较采用单因素方差分析(One-Way ANOVA), 若发现存在显著性差异, 则进一步使用SNK-*q*检验进行组间两两比较。以$P<0.05$判定差异具有统计学意义。

2 结果

2.1 MIR17HG和miR-153-3p在癌组织和细胞中的表达水平比较

MM组织中MIR17HG表达水平高于正常骨髓组织, miR-153-3p表达水平低于正常骨髓组织($P<0.05$); MM细胞系U266、NCI-H929、RPMI-8226和LP-1中MIR17HG表达水平高于nPCs细胞, miR-153-3p表达水平低于nPCs细胞($P<0.05$)。选择基因表达变化最显著的NCI-H929细胞为后续实验细胞。见表1和表2。

2.2 MIR17HG和miR-153-3p在各组NCI-H929细胞中的表达比较

在si-MIR17HG组NCI-H929细胞中, MIR17HG表达水平低于control组和si-NC组, miR-153-3p表达水平高于control组和si-NC组($P<0.05$); 在si-MIR17HG+miR-153-3p inhibitor组NCI-H929细胞中, miR-153-3p表达水平比si-MIR17HG+inhibitor NC组低($P<0.05$); si-MIR17HG+miR-153-3p mimics组

NCI-H929细胞相较于si-MIR17HG+miR-NC组miR-153-3p表达水平升高(P<0.05)。见表3。

2.3 各组NCI-H929细胞中增殖活力比较

在si-MIR17HG组NCI-H929细胞中, D_{450}(24 h、48 h)值低于Control组和si-NC组(P<0.05); 在si-MIR17HG+miR-153-3p inhibitor组NCI-H929细胞中, D_{450}(24 h、48 h)值高于si-MIR17HG+inhibitor NC组(P<0.05); 在si-MIR17HG+miR-153-3p mimics组NCI-H929细胞中, D_{450}(24 h、48 h)值低于si-MIR17HG+miR-NC组(P<0.05)。见表4。

2.4 各组NCI-H929细胞迁移和侵袭能力比较

相较于control组和si-NC组, si-MIR17HG组NCI-H929细胞中细胞划痕愈合率和侵袭数量降低(P<0.05); si-MIR17HG+miR-153-3p inhibitor组NCI-H929细胞中上述指标水平高于si-MIR17HG+inhibitor NC组(P<0.05); 在si-MIR17HG+miR-153-3p mimics组NCI-H929细胞中, 细胞划痕愈合率和侵袭数量相较于si-MIR17HG+miR-NC组降低(P<0.05)。见图1、图2和表5。

2.5 各组NCI-H929细胞凋亡率比较

在si-MIR17HG组NCI-H929细胞中, 凋

表1 MM组织和正常骨髓组织中MIR17HG和miR-153-3p表达比较

Table 1 Comparison of expression levels of MIR17HG and miR-153-3p in MM tissues and normal bone marrow tissues

组别 Group	MIR17HG	miR-153-3p
Normal bone marrow tissue	1.01±0.00	1.00±0.00
MM tissue	1.92±0.05*	0.32±0.01*

*P<0.05, 与正常骨髓组织组比较。$\bar{x}\pm s$, n=26。

*P<0.05 compared with normal bone marrow tissue group. $\bar{x}\pm s$, n=26.

表2 MIR17HG和miR-153-3p在人正常骨髓浆细胞和MM细胞中表达比较

Table 2 Comparison of expression of MIR17HG and miR-153-3p in normal human bone marrow plasma cells and MM cells

组别 Group	MIR17HG	miR-153-3p
nPCs	1.00±0.00	1.00±0.00
U266	1.83±0.09*	0.37±0.03*
NCI-H929	2.26±0.11*	0.31±0.03*
RPMI-8226	1.92±0.09*	0.43±0.05*
LP-1	2.04±0.08*	0.48±0.05*

*P<0.05, 与nPCs细胞组比较。$\bar{x}\pm s$, n=26。

*P<0.05 compared with nPCs cells group. $\bar{x}\pm s$, n=26.

表3 MIR17HG和miR-153-3p在各组NCI-H929细胞中表达比较

Table 3 Comparison of expression levels of MIR17HG and miR-153-3p of NCI-H929 cells in each group

组别 Group	MIR17HG	miR-153-3p
Control	1.00±0.00	1.00±0.00
si-NC	1.00±0.01	1.00±0.01
si-MIR17HG	0.34±0.03*#	1.87±0.09*#
si-MIR17HG+inhibitor NC	0.33±0.03	1.86±0.10
si-MIR17HG+miR-153-3p inhibitor	0.32±0.03	1.39±0.05&
si-MIR17HG+miR-NC	0.33±0.02	1.88±0.09
si-MIR17HG+miR-153-3p mimics	0.34±0.03	2.25±0.14△

*P<0.05, 与control组比较; #P<0.05, 与si-NC组比较; &P<0.05, 与si-MIR17HG+inhibitor NC组比较; △P<0.05, 与si-MIR17HG+miR-NC组比较。$\bar{x}\pm s$, n=6。

*P<0.05 compared with control group; #P<0.05 compared with si-NC group; &P<0.05 compared with si-MIR17HG+inhibitor NC group; △P<0.05 compared with si-MIR17HG+miR-NC group. $\bar{x}\pm s$, n=6.

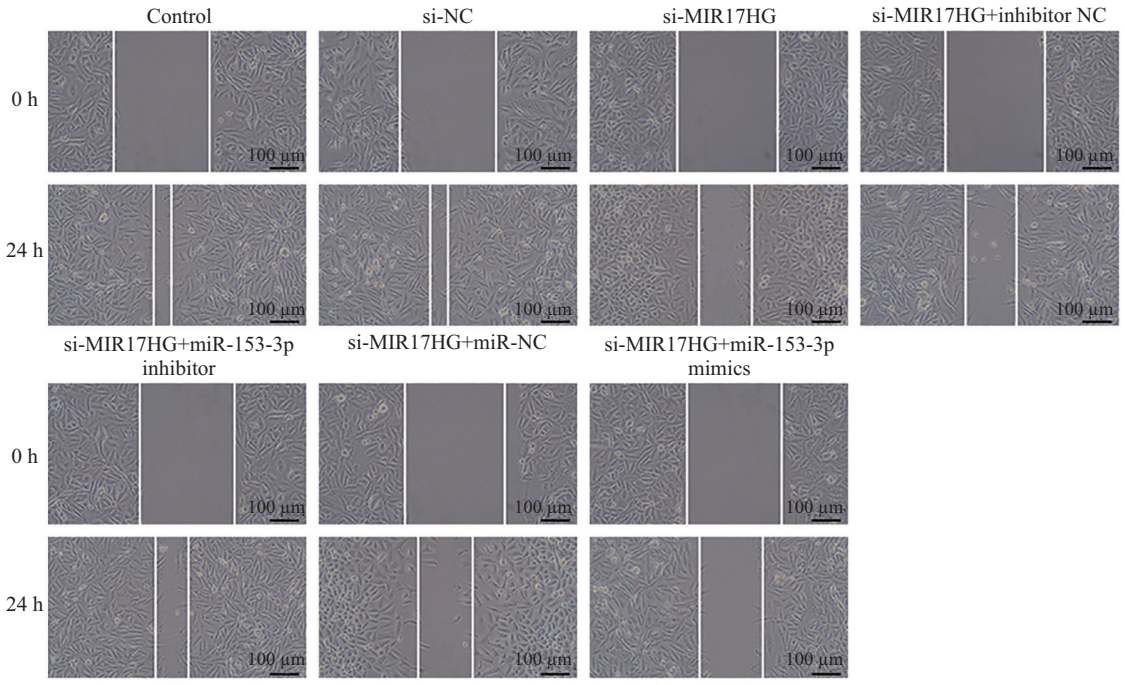

图1 MIR17HG与miR-153-3p对NCI-H929细胞迁移能力的影响

Fig.1 The effects of MIR17HG and miR-153-3p on the migration ability of NCI-H929 cells

表4 各组NCI-H929细胞中增殖活力比较

Table 4 Comparison of proliferation activity among different groups of NCI-H929 cells in each group

组别 Group	D_{450}	
	24 h	48 h
Control	0.38±0.03	0.78±0.06
si-NC	0.37±0.03	0.76±0.05
si-MIR17HG	0.25±0.02*#	0.51±0.04*#
si-MIR17HG+inhibitor NC	0.26±0.02	0.52±0.04
si-MIR17HG+miR-153-3p inhibitor	0.31±0.03&	0.65±0.05&
si-MIR17HG+miR-NC	0.25±0.03	0.53±0.04
si-MIR17HG+miR-153-3p mimics	0.18±0.02△	0.40±0.03△

*P<0.05, 与control组比较; #P<0.05, 与si-NC组比较; &P<0.05, 与si-MIR17HG+inhibitor NC组比较; △P<0.05, 与si-MIR17HG+miR-NC组比较。$\bar{x}\pm s$, n=6。

*P<0.05 compared with control group; #P<0.05 compared with si-NC group; &P<0.05 compared with si-MIR17HG+inhibitor NC group; △P<0.05 compared with si-MIR17HG+miR-NC group. $\bar{x}\pm s$, n=6.

亡率高于control组和si-NC组(P<0.05); 在si-MIR17HG+miR-153-3p inhibitor组NCI-H929细胞中, 凋亡率低于si-MIR17HG+inhibitor NC组(P<0.05); 在si-MIR17HG+miR-153-3p mimics组NCI-H929细胞中, 凋亡率高于si-MIR17HG+miR-NC组(P<0.05)。见图3和表6。

2.6 各组NCI-H929细胞相关蛋白表达比较

NCI-H929细胞N-cadherin、vimentin、PCNA和MMP-2蛋白表达水平比较: si-MIR17HG组低于control组和si-NC组(P<0.05), si-MIR17HG+miR-153-3p inhibitor组高于si-MIR17HG+inhibitor NC组(P<0.05), si-MIR17HG+miR-153-3p mimics组低于si-MIR17HG+miR-NC组(P<0.05); E-cadherin和cleaved caspase-3蛋白表达水平比较: si-MIR17HG组高于control组和si-NC组(P<0.05), si-MIR17HG+miR-153-3p inhibitor组低于si-MIR17HG+inhibitor NC组(P<0.05), si-MIR17HG+miR-153-3p mimics组高于si-MIR17HG+miR-NC组(P<0.05)。见图4和表7。

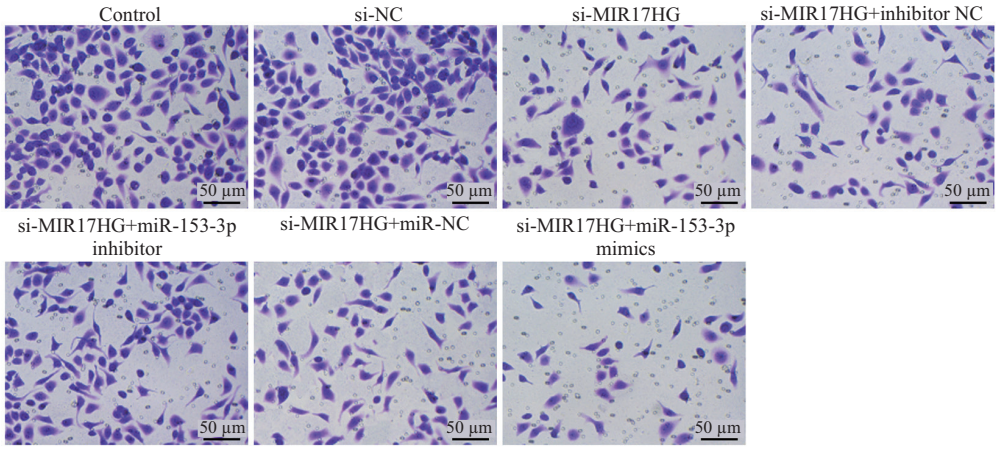

图2 MIR17HG与miR-153-3p对NCI-H929细胞侵袭能力的影响

Fig.2 The effects of MIR17HG and miR-153-3p on the invasion ability of NCI-H929 cells

表5 各组NCI-H929细胞迁移和侵袭能力比较

Table 5 Migration and invasion of NCI-H929 cells in each group

组别 Group	划痕愈合率/% Scratch healing rate /%	侵袭数量 Invasion quantity
Control	80.56±7.42	179.48±23.64
si-NC	82.14±7.63	176.52±22.37
si-MIR17HG	46.62±3.51*#	67.61±9.42*#
si-MIR17HG+inhibitor NC	48.73±3.85	68.74±9.53
si-MIR17HG+miR-153-3p inhibitor	65.48±6.24&	126.35±17.81&
si-MIR17HG+miR-NC	47.38±4.16	69.27±8.76
si-MIR17HG+miR-153-3p mimics	32.95±4.78△	42.19±6.05△

*P<0.05, 与control组比较; #P<0.05, 与si-NC组比较; &P<0.05, 与si-MIR17HG+inhibitor NC组比较; △P<0.05, 与si-MIR17HG+miR-NC组比较。$\bar{x}\pm s$, n=6。

*P<0.05 compared with control group; #P<0.05 compared with si-NC group; &P<0.05 compared with si-MIR17HG+inhibitor NC group; △P<0.05 compared with si-MIR17HG+miR-NC group. $\bar{x}\pm s$, n=6.

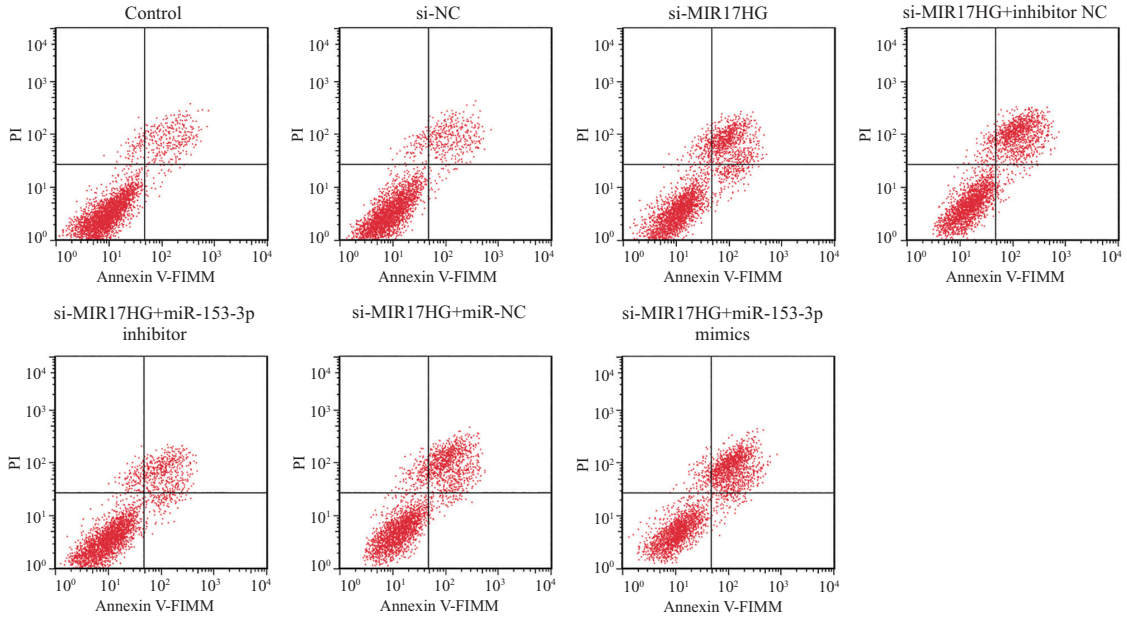

图3 MIR17HG与miR-153-3p对NCI-H929细胞凋亡的影响

Fig.3 The effects of MIR17HG and miR-153-3p on apoptosis of NCI-H929 cells

表6 各组NCI-H929细胞凋亡率比较

Table 6 Comparison of apoptosis rates of NCI-H929 cells in each group

组别 Group	凋亡率/% Apoptosis rate /%
Control	3.91±0.47
si-NC	4.12±0.56
si-MIR17HG	35.87±4.32*#
si-MIR17HG+inhibitor NC	37.13±4.18
si-MIR17HG+miR-153-3p inhibitor	18.26±2.47&
si-MIR17HG+miR-NC	34.95±4.01
si-MIR17HG+miR-153-3p mimics	46.54±4.39△

*P<0.05, 与control组比较; #P<0.05, 与si-NC组比较; &P<0.05, 与si-MIR17HG+inhibitor NC组比较; △P<0.05, 与si-MIR17HG+miR-NC组比较。$\bar{x}\pm s$, n=6。

*P<0.05 compared with control group; #P<0.05 compared with si-NC group; &P<0.05 compared with si-MIR17HG+inhibitor NC group; △P<0.05 compared with si-MIR17HG+miR-NC group. $\bar{x}\pm s$, n=6.

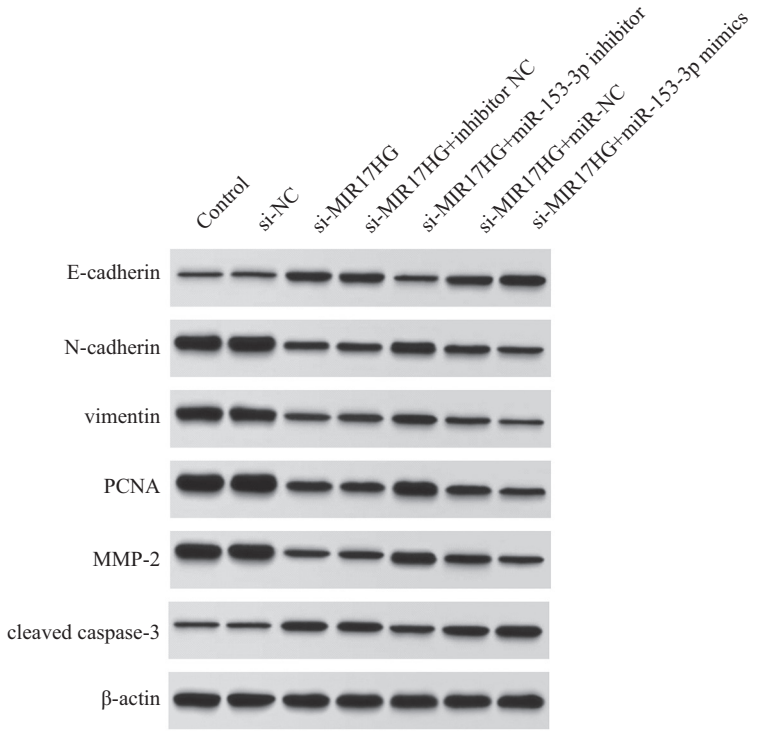

图4 E-cadherin、N-cadherin、vimentin、PCNA、MMP-2、cleaved caspase-3蛋白表达电泳图

Fig.4 Electrophoretogram of E-cadherin, N-cadherin, vimentin, PCNA, MMP-2, and cleaved caspase-3 protein expression

2.7 验证miR-153-3p与MIR17HG的靶向关系

图6所示为miR-153-3p与MIR17HG的结合位点(Starbase网站)。miR-153-3p mimics+MIR17HG-WT组相较于miR-NC+MIR17HG-WT组荧光素酶活性降低(P<0.05), 见表7。

3 讨论

MM是一种由骨髓中浆细胞过度增殖引起的血液系统恶性肿瘤, 其发病率呈逐年持续上升趋势, 约占所有人类癌症的1%[10]。尽管MM的临床诊疗取得一定进展, 新的治疗靶点也不断发现, 但MM的临床治疗效果仍然不佳, 5年总生存率处于较低水平[11]。因此, 深入解析关键分子的调控网络对于改善MM的诊断精准度与治疗有效性具有重要意义[12]。

研究显示, LncRNA的异常表达与包括多发性骨髓瘤在内的各类肿瘤的发生和预后密切相关[13]。邓幻苏等[14]研究显示, MIR17HG在宫颈癌组织和细胞中高表达, 敲低MIR17HG表达可抑制宫颈癌细胞生

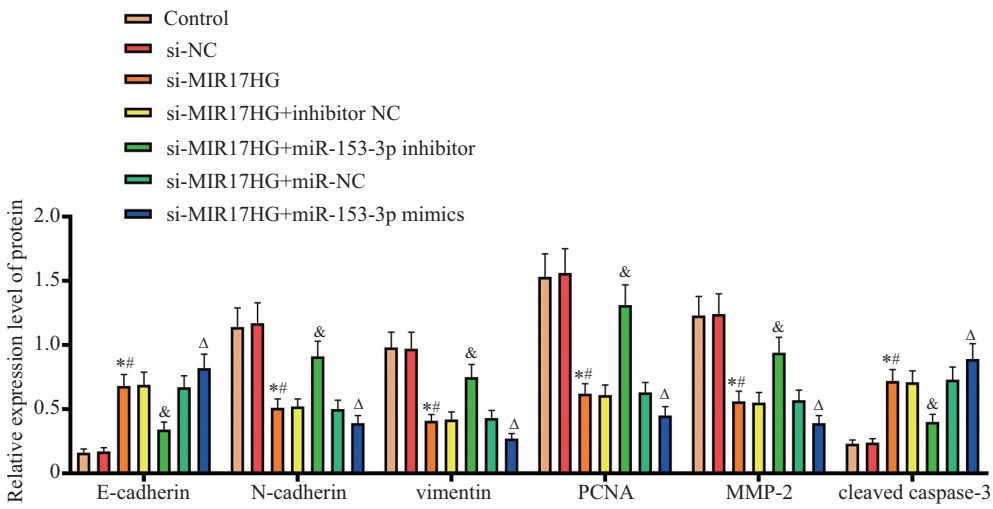

*P<0.05, 与control组比较; #P<0.05, 与si-NC组比较; &P<0.05, 与si-MIR17HG+inhibitor NC组比较; △P<0.05, 与si-MIR17HG+miR-NC组比较。$\bar{x}\pm s$, n=6。

*P<0.05 compared with control group; #P<0.05 compared with si-NC group; &P<0.05 compared with si-MIR17HG+inhibitor NC group; △P<0.05 compared with si-MIR17HG+miR-NC group. $\bar{x}\pm s$, n=6.

图5 各组NCI-H929细胞E-cadherin、N-cadherin、vimentin、PCNA、MMP-2、cleaved caspase-3蛋白表达水平比较

Fig.5 Comparison of protein expression levels of E-cadherin, N-cadherin, vimentin, PCNA, MMP-2, and cleaved caspase-3 of NCI-H929 cells in each group

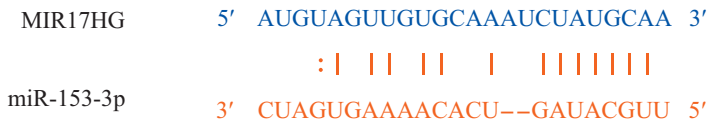

图6 miR-153-3p与MIR17HG的靶向结合位点

Fig.6 The targeted binding sites of miR-153-3p and MIR17HG

表7 miR-153-3p与MIR17HG的靶向关系验证

Table 7 Experimental validation of MIR17HG targeting miR-153-3p

组别 Group	荧光素酶活性 Luciferase activity
miR-NC+MIR17HG-WT	1.04±0.05
miR-153-3p mimics+MIR17HG-WT	0.39±0.03*
miR-NC+MIR17HG-MUT	1.05±0.06
miR-153-3p mimics+MIR17HG-MUT	1.08±0.09

*P<0.05, 与miR-NC+MIR17HG-WT相比。$\bar{x}\pm s$, n=6。

*P<0.05 compared with miR-NC+MIR17HG-WT. $\bar{x}\pm s$, n=6.

物学活性。MIR17HG在视网膜瘤中发挥促癌功能，其表达下调可显著削弱细胞的恶性行为[15]。本研究中，MM组织和细胞系中MIR17HG呈高表达，与既往MIR17HG在肿瘤中发挥促癌作用的研究结论一致，提示MIR17HG可能参与MM的发病进程。

上皮–间质转化(epithelial-mesenchymal transition, EMT)是驱动肿瘤恶性进展的关键步骤，该过程使癌细胞获得迁移与侵袭等新的功能特性; E-cadherin作为上皮细胞标志性蛋白，其表达水平降低会破坏细胞间紧密连接、削弱上皮细胞极性; N-cadherin与vimentin是间质细胞的关键标志物，其表达水平上调与细胞迁移、侵袭能力的增强直接相关[16]; 细胞外基质是肿瘤细胞迁移的物理屏障，MMP-2蛋白可降解细胞外基质中IV和V型胶原蛋白，破坏细胞外基质完整性，促进肿瘤细胞迁移[17]。在本研究中，敲低MIR17HG可通过调控EMT相关蛋白(N-cadherin、vimentin、

MMP-2、E-cadherin)的表达，进而抑制视网膜瘤细胞的迁移与侵袭。这表明MIR17HG可通过调控EMT过程影响NCI-H929细胞迁移和侵袭。

骨髓瘤细胞具有高增殖和低凋亡的生理特性，PCNA是细胞周期进展的关键蛋白，参与DNA复制和修复过程，其高表达与肿瘤细胞增殖活性增强密切相关[18]；cleaved caspase-3是凋亡通路的核心效应分子，可识别并切割多种细胞内底物，破坏细胞结构和功能，诱导细胞发生凋亡[19]。在本研究中，敲低MIR17HG可通过调控PCNA和cleaved caspase-3表达水平，来抑制NCI-H929细胞增殖，促进其凋亡，增殖和凋亡实验证实该结论。这提示敲低MIR17HG表达可抑制MM细胞生物学活性。

LncRNA能够作为分子海绵吸附miRNA，通过此方式解除miRNA对其靶基因的抑制，最终影响肿瘤细胞的生物学功能[7]。Starbase网站预测分析发现MIR17HG与miR-153-3p存在靶向结合位点。JIA等[20]研究表明miR-153-3p过表达可抑制胃癌细胞增殖和转移。YANG等[21]研究表明miR-153-3p在鳞状细胞癌中低表达，过表达miR-153-3p可抑制胃癌细胞迁移和侵袭。推测miR-153-3p对肿瘤细胞具有一定的抑制作用。在本研究中，MM组织和细胞系中miR-153-3p在表达水平明显下调，与前人研究结果研究一致。敲低MIR17HG表达可显著上调miR-153-3p表达水平，回复实验结果显示，沉默miR-153-3p表达可降低下调MIR17HG表达对NCI-H929细胞的抑制作用。过表达miR-153-3p可进一步强化由MIR17HG敲低所引发的对NCI-H929细胞恶性行为的抑制效应。以上结果提示MIR17HG可通过海绵化miR-153-3p表达来调控NCI-H929细胞生物学活性。

综上所述，敲低MIR17HG表达可通过促进miR-153-3p表达来抑制NCI-H929细胞恶性生物学行为。miR-153-3p如何调控其下游mRNA表达来影响NCI-H929细胞生物学活性，本研究未做探讨，后续还需进一步研究。

参考文献 (References)

[1] CORTES-SELVA D, PEROVA T, SKERGET S, et al. Correlation of immune fitness with response to teclistamab in relapsed/refractory multiple myeloma in the MajesTEC-1 study [J]. Blood, 2024, 144(6): 615-28.

[2] SHEN Q, JIANG Q, CONG Z, et al. Knockdown of lncRNA AL928768.3 inhibits multiple myeloma cell proliferation by inducing cell cycle arrest in G_0/G_1 phase [J]. Ann Transl Med, 2022, 10(4): 172-82.

[3] GRILLONE K, ASCRIZZI S, CREMASCHI P, et al. An unbiased lncRNA dropout CRISPR-Cas9 screen reveals RP11-350G8.5 as a novel therapeutic target for multiple myeloma [J]. Blood, 2024, 144(16): 1705-21.

[4] AL-HAWARY S I S, JASIM S A, ALTALBAWY F M A, et al. Highlighting the role of long non-coding RNA (LncRNA) in multiple myeloma (MM) pathogenesis and response to therapy [J]. Med Oncol, 2024, 41(7): 171-82.

[5] MORELLI E, FULCINITI M, SAMUR M K, et al. A MIR17HG-derived long noncoding RNA provides an essential chromatin scaffold for protein interaction and myeloma growth [J]. Blood, 2023, 141(4): 391-405.

[6] ZHENG G, YE H, BAI J, et al. Downregulation of lncRNA MIR17HG reduced tumorigenicity and Treg-mediated immune escape of non-small-cell lung cancer cells through targeting the miR-17-5p/RUNX3 axis [J]. J Biochem Mol Toxicol, 2024, 38(5): e23715-26.

[7] XU Y, WANG T, WAN J, et al. Long non-coding RNA NEAT1 promotes multiple myeloma malignant transformation via targeting miR-485-5p/ABCB8 [J]. Hematology, 2024, 29(1): 2422153-62.

[8] 杨楠, 徐保华, 袁志丽. miR-153-3p通过靶向ACTN4调节食管癌细胞的恶性生物学行[J]. 现代免疫学(YANG N, XU B H, YUAN Z L. miR-153-3p regulates the malignant biological behavior of esophageal cancer cells by targeting ACTN4 [J]. Modern Immunology), 2024, 44(2): 112-20.

[9] DENG X, GUO B, FAN Y. MiR-153-3p suppresses cell proliferation, invasion and glycolysis of thyroid cancer through inhibiting E3F3 expression [J]. Onco Targets Ther, 2021, 14(3): 519-29.

[10] CHU M, FAN Y, WU L, et al. Knockdown of lncRNA BDNF-AS inhibited the progression of multiple myeloma by targeting the miR-125a/b-5p-BCL2 axis [J]. Immun Ageing, 2022, 19(1): 3-14.

[11] YANG X, HUANG H, WANG X, et al. Knockdown of lncRNA SNHG16 suppresses multiple myeloma cell proliferation by sponging miR-342-3p [J]. Cancer Cell Int, 2020, 20(3): 38-49.

[12] WANG Q M, LIAN G Y, SHENG S M, et al. Exosomal lncRNA NEAT1 inhibits NK-cell activity to promote multiple myeloma cell immune escape via an EZH2/PBX1 axis [J]. Mol Cancer Res, 2024, 22(2): 125-36.

[13] NING J, YANG R, WANG H, et al. LncRNA MALAT1 silencing represses CXCL12-induced proliferation, invasion, and homing behavior in multiple myeloma by inhibiting CXCR4 [J]. Hematology, 2024, 29(1): 2422154.

[14] 邓幻苏, 刘元斌. 过表达lncRNA MIR17HG促进宫颈癌HeLa细胞的恶性生物学行为与裸鼠移植瘤生长[J]. 中国肿瘤生物治疗杂志(DENG H S, LIU Y B. Overexpression of lncRNA MIR17HG promotes the malignant biological behavior of cervical cancer HeLa cells and the growth of transplanted tumors in nude mice [J]. Chinese Journal of Tumor Biotherapy), 2022, 29(8): 741-9.

[15] YAN J, DENG Y X, CAI Y L, et al. LncRNA MIR17HG promotes the proliferation, migration, and invasion of retinoblastoma cells by up-regulating HIF-1α expression via sponging miR-155-5p [J]. Kaohsiung J Med Sci, 2022, 38(6): 554-64.

[16] FAN B, WANG L, WANG J. RAB22A as a predictor of exosome secretion in the progression and relapse of multiple myeloma [J]. Aging, 2024, 16(5): 4169-90.

[17] GUI H, FAN X. Anti-tumor effect of dandelion flavone on multiple myeloma cells and its mechanism [J]. Discov Oncol, 2024, 15(1): 215-26.

[18] VASHIST A, GUPTA N, NAFEES S, et al. Habb-e-asgandh suppresses cell proliferation and induces apoptosis through mitochondria dysfunction in multiple myeloma cells [J]. Asian Pac J Cancer Prev, 2022, 23(11): 3629-39.

[19] SUN R J, XU J, GAO W, et al. Effect of guizhi fuling capsule on apoptosis of myeloma cells through mitochondrial apoptosis pathway [J]. Chin J Integr Med, 2023, 29(2): 127-36.

[20] JIA Z, TANG X, ZHANG X, et al. miR-153-3p attenuates the development of gastric cancer by suppressing SphK2 [J]. Biochem Genet, 2022, 60(5): 1748-61.

[21] YANG W, CHEN Y. LncRNA TEX41 promotes the proliferation and migration of squamous cell carcinoma cells by upregulating Atg5 via sponging miR-153-3p [J]. Cell Mol Biol, 2023, 69(14): 248-54.